AGU PUBLICATIONS

JGR

Journal of Geophysical Research: Oceans

RESEARCH ARTICLE

10.1002/2016JC012507

Key Points:
- Lidar and MBES data were combined to provide thorough coverage of coral reef
- Robust estimation and depth calibration were introduced to obtain an accurate estimate of terrain complexity in coral reef environments
- Derived terrain complexity index was found to be significantly correlated with in situ observation of coral abundance

Correspondence to:
F. Yang,
flyang@126.com

Citation:
Zhang, K., F. Yang, H. Zhang, D. Su, and Q.Q. Li (2017), Morphological characterization of coral reefs by combining lidar and MBES data: A case study from Yuanzhi Island, South China Sea , *J. Geophys. Res. Oceans*, *122*, 4779–4790, doi:10.1002/2016JC012507.

Received 25 OCT 2016
Accepted 10 MAY 2017
Accepted article online 16 MAY 2017
Published online 13 JUN 2017

Morphological characterization of coral reefs by combining lidar and MBES data: A case study from Yuanzhi Island, South China Sea

Kai Zhang[1,2], Fanlin Yang[1,2], Hande Zhang[3], Dianpeng Su[1], and QianQian Li[1,2]

[1]College of Geomatics, Shandong University of Science and Technology, Qingdao, China, [2]Key Laboratory of Surveying and Mapping Technology on Island and Reef, National Administration of Surveying, Mapping and Geoinformation, Qingdao, China, [3]Northern Sea Airborne Detachment, China Marine Surveillance, Qingdao, China

Abstract The correlation between seafloor morphological features and biological complexity has been identified in numerous recent studies. This research focused on the potential for accurate characterization of coral reefs based on high-resolution bathymetry from multiple sources. A standard deviation (STD) based method for quantitatively characterizing terrain complexity was developed that includes robust estimation to correct for irregular bathymetry and a calibration for the depth-dependent variablity of measurement noise. Airborne lidar and shipborne sonar bathymetry measurements from Yuanzhi Island, South China Sea, were merged to generate seamless high-resolution coverage of coral bathymetry from the shoreline to deep water. The new algorithm was applied to the Yuanzhi Island surveys to generate maps of quantitive terrain complexity, which were then compared to in situ video observations of coral abundance. The terrain complexity parameter is significantly correlated with seafloor coral abundance, demonstrating the potential for accurately and efficiently mapping coral abundance through seafloor surveys, including combinations of surveys using different sensors.

1. Introduction

Coral reefs are facing serious stress and declining worldwide, owing to the combined effects of natural and anthropogenic threats [*Hedley et al.*, 2016]. Due to the magnitude of these threats, monitoring coral reef ecosystems, which is an essential step in assessing the impact of disturbances on reefs and tracking their subsequent recoveries, has drawn increasing attention in recent years. In particular, the mapping of coral abundance levels on the seafloor can provide valuable information about the trends of coral variation and has thus become an increasingly popular topic of research.

Traditionally, the coral abundance status is determined from time consuming and inconvenient in situ observations. A variety of remote sensing approaches have been explored over the last two decades to obtain a cost-effective measurement of coral abundance [*Mishra et al.*, 2007; *Reshitnyk et al.*, 2014; *Hedley et al.*, 2016]. Among these methods, the combination of a multibeam echo sounders system (MBES) and light detection and ranging (lidar) technology has received much attention recently owing to its improved resolution and coverage [*Costa et al.*, 2009; *Ierodiaconou et al.*, 2011; *Micallef et al.*, 2012; *Kennedy et al.*, 2014; *Young et al.*, 2015]. MBES has become the preferred approach for seafloor mapping because of its ability to provide high-resolution measurements across a variety of depths (a few to several thousand meters), has become the preferred approach for seafloor mapping [*Anderson et al.*, 2008; *Zieger et al.*, 2009; *Lurton*, 2010]. However, in coral reef environments, a large portion of the seafloor is located in very shallow-water region ($<$5 m), which is too shallow for the safe operation of MBES. In the region where MBES is inoperable, lidar is a convenient alternative option [*Wang and Philpot*, 2007; *Wedding et al.*, 2008; *Collin et al.*, 2012; *Tulldahl et al.*, 2012; *Yamamoto et al.*, 2012; *Zavalas et al.*, 2014; *Brock and Purkis*, 2015]. lidar can provide high-resolution seafloor data (on the order of meters) for depths ranging from around 1 m to several tens of meters, depending on the clarity of the water, and is cost-effective [*Costa et al.*, 2009]. Obviously, these two methods are complementary in terms of their survey scope. Thus, by combining these two methods, an approximately seamless measurement of a coral reef can be obtained, resulting in a high-resolution data set across a large range of depths. Using these data, there is the potential for a better characterization of coral reef systems.

Aside from considerations of the resolution and coverage of the data, the main concern of this area of study is how to better characterize coral abundance based on the seafloor measurements acquired. In this respect, terrain complexity is a reasonable proxy for coral abundance owing to the evident relationship between bathymetric terrain complexity and benthic habitat biodiversity [*Brock et al*., 2006; *Collier and Humber*, 2007; *Pittman et al*., 2011; *Lecours et al*., 2016a,2016b; *Hedley et al*., 2016]. Following the recognition of such a link, terrain complexity has increasingly been viewed as an important indicator with a coral mapping application [*Hedley et al*., 2016]. However, two problems prevent an accurate measurement of the terrain complexity of a coral reef, and few studies have been conducted to address these problems. First, the bathymetry of the coral reef is highly variable and irregular, which often prevents an accurate measurement of the terrain complexity level. Second, the measurement noise in bathymetric data is similar to actual seafloor complexity signals. Moreover, due to the inherent depth-dependent pattern of the noise, significant disturbances may occur in the computational results. Thus, if not properly addressed, both of these factors could result in seriously biased results of terrain complexity. Consequently, the statistical relationship between the coral abundance and terrain complexity will be distorted.

Aside from considerations of the resolution and coverage of the data, the main concern of this area of study is how to better characterize coral abundance based on the seafloor mapping data. To this end, this study focused on the impacts of irregular bathymetry as well as the depth-dependent pattern of the measurement uncertainty. The goals of this study include the following: (1) research the accurate measurement of terrain complexity in a coral reef environment and (2) evaluate the statistical relationship between terrain complexity and coral abundance.

2. Study Area

The study area is the Xisha Archipelago, which is located in the northern part of the South China Sea (Figure 1a). Due to its distance from the mainland, the marine environment in this area is in relatively pristine condition. In recent years, the pollution in this region has increased as a consequence of the growing disturbance of human activity [*Xu et al*., 2011]. To mitigate the environmental risks, China's government has imposed restrictions on travel to this area. Meanwhile, the response of the local marine environment has drawn increasing attention.

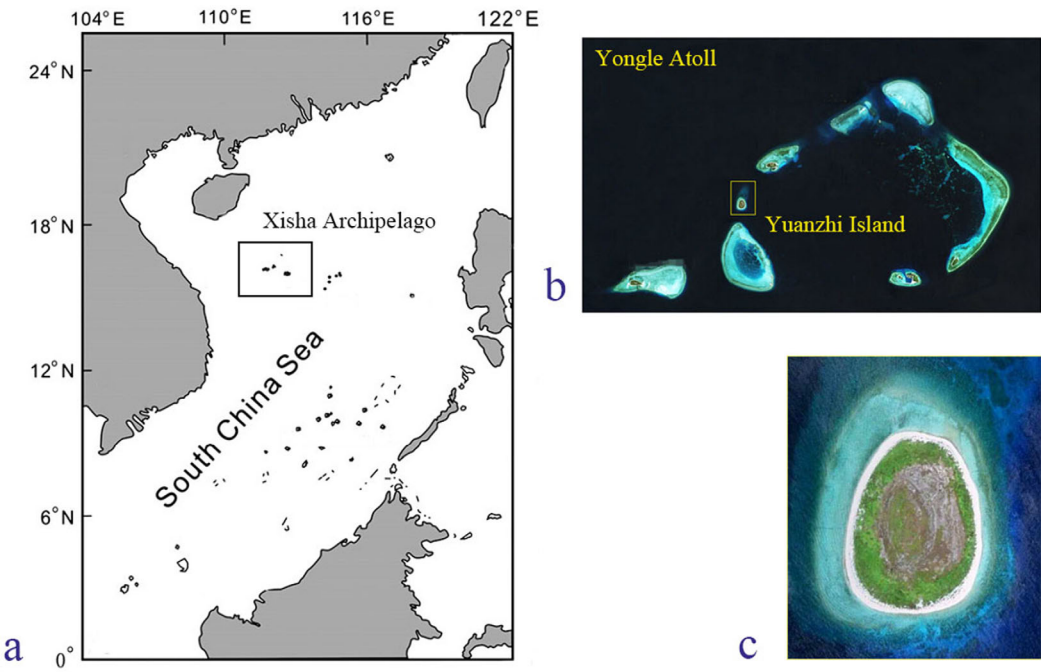

Figure 1. (a) Location of the Xisha Archipelago. (b) Satellite image of the Yongle Atoll. (c) Satellite image of Yuanzhi Island.

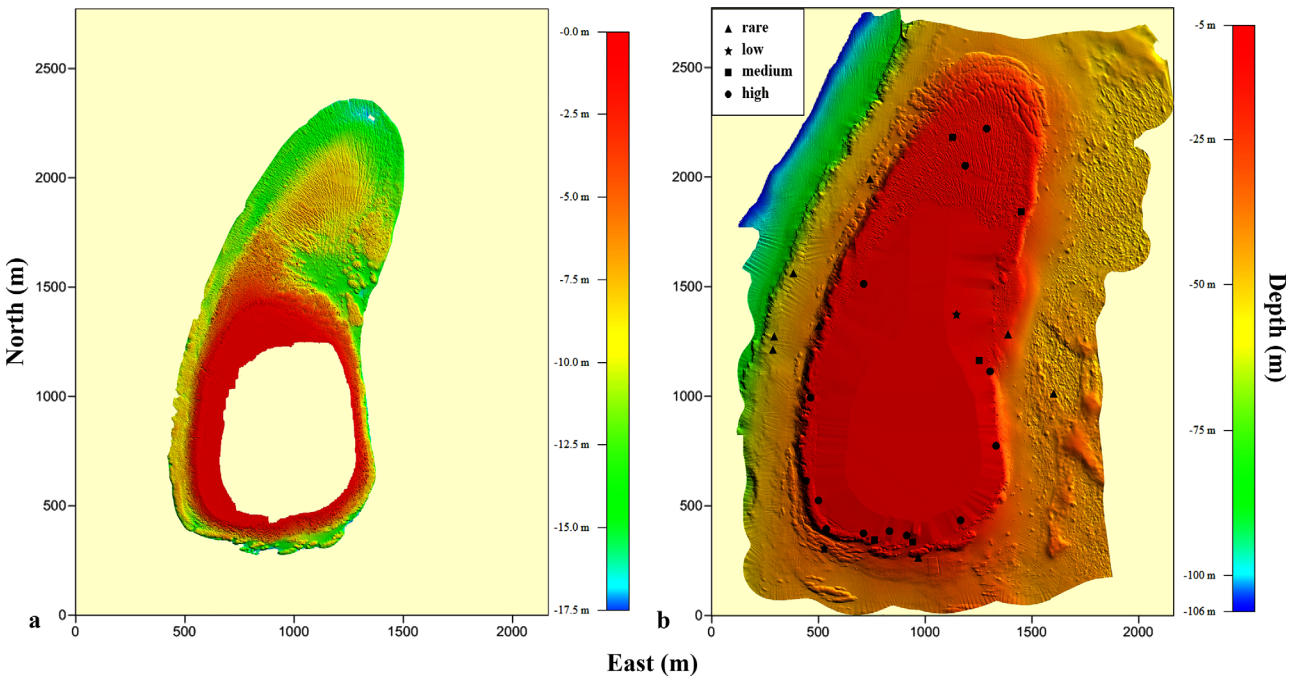

Figure 2. (a) Shaded relief image generated with lidar data. (b) Shaded relief image generated with MBES data and horizontal locations of ground-truth data with different coral abundance levels (triangle-rare; star-low; square-medium; circular-high).

Yuanzhi Island (Figure 1c), with an area of approximately 0.3 km^2, is a typical coral islet located in the Yongle Atoll (a major part of the Xisha Archipelago). As shown in Figure 1b, Yuanzhi Island is located at the edge of the atoll. Consequently, the depth of the seafloor changes drastically along the western edge of the island (reaching 100 m at locations 1 km offshore). Therefore, to seamlessly characterize the coral reef in such a variable bathymetric environment, bathymetric data collected with lidar and MBES equipment s were used in this study.

Lidar measurements were collected at Yuanzhi Island in January 2013. In this survey, the shallow part of the bathymetry was measured with an airborne Optech Aquarius system operated at an altitude of approximately 300 m. During the survey, a POS AV 510 navigation system was used to provide the horizontal position with an accuracy of 1.5–3 m. The real-time position and attitude data were obtained via the Applanix POSPac MMS software. The raw lidar data were processed by waveform extraction, multisource data fusion, refraction correction, and other steps with the Optech LMS software. In addition, the processing steps including filtering points, mosaicking raw strips, and gridding data were performed with TerraScan software. In the end, more than 1.8×10^8 laser shots with the LAS format were acquired in the experimental area. Through visual judgment, it was recognized that the system provided a credible survey only when the depth was shallower than 17 m due to the turbidity status of the seawater. After removing the outliers by manual editing, a point cloud data set with a density of approximately 3 point/m^2 was obtained. Afterward, a gridded DEM with a resolution of 1 m was generated by linearly interpolating the point cloud (with Golden Surfer 11.0 software) (Figure 2a).

For the deeper region where lidar was prohibited, the seafloor was measured with MBES in May 2016. A high-resolution shallow-water MBES, R2SONIC 2024, was used for the data collection. In the survey, the horizontal position of the sonar was measured with a dual-frequency differential GPS, which provided centimeter horizontal positioning precision. To guarantee the horizontal coverage rate, the spacing between adjacent survey lines was adjusted according to the depth to provide a varying 40–70% overlap. In addition, sound velocity data were measured with a CTD logger (Ocean Seven304), and tide information was measured by an AML tidal gauge. The collected data were processed with the CARIS HISP/SISP 9.1 package to obtain the bathymetric data. After manually editing outliers, the bathymetric data were gridded into a XYZ format with a 1 m horizontal resolution (with the Golden Surfer 11.0 software, using the "triangulation with linear interpolation" method) (Figure 2b). In the nearshore region of the island, no MBES data were available

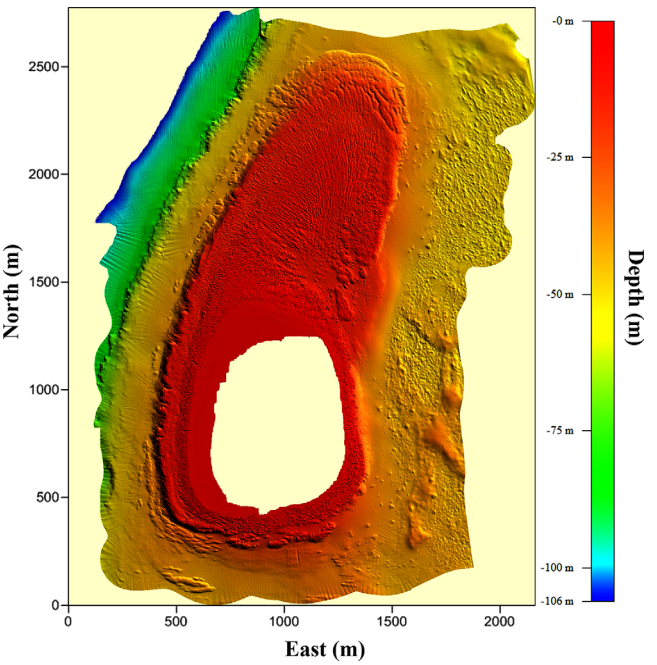

Figure 3. Shaded relief image generated with the merged data.

because the water was too shallow for the boat to access safely. Thus, only isolated depth measurements could be collected in this region using a single-beam echo sounder that was mounted on a dinghy. With this low-resolution information, the shape of the seafloor can only be roughly depicted and cannot be used to characterize the seafloor in detail. However, this region is one of particular interest to habitat researchers because an abundance of coral was found in this area. Therefore, bathymetric data collected with both lidar and MBES equipment were required to acquire full and seamless coverage of the coral reef.

To achieve such a combination, the two data sets were merged to produce a combined data set. In the merging process, the vertical reference frames of the two data sets were unified according to the tidal measurements. Afterward, gaps in the MBES survey area were filled with lidar data. There were two major concerns when merging these two data sets. First, there was a temporal gap (of approximately 4.5 years) between the two data sets, which inevitably introduced some inconsistency between the bathymetric data from the two different sources. Second, for the morphological analysis in this study, it was critical to retain the neighboring consistency of the bathymetric data in each local window. Hence, instead of simply filling in the discrete gaps in the MBES data set, the lidar data with depths above 14.5 m were considered as a whole to represent the bathymetric information in the merged data set. The bathymetry of the integrated data set was given in Figure 3. The area of the merged data was approximately 2.7 km by 2.1 km, with depths ranging from less than 1 m to over 100 m. Obviously, the combination of the two data sets provided thorough coverage of the study area. However, the figure also shows that there was a small vertical gap between the two different data sets. The histogram of the vertical differences between the MBES and lidar data on the merging edge is given in Figure 4. The distribution of the difference is a roughly bell shape, but not a standard Gaussian distribution shape. The median value and the median absolute deviation (MAD) of the difference were determined to be 0.08 m and 0.28 m, respectively. This vertical gap is attributed not only to the temporal gap of the two data sets but also to the potential errors in the bathymetric and tidal measurements.

In addition to the bathymetric data, in situ observations of the coral abundance on the seafloor were also collected. Specifically, field documentation of the bottom substrate was made using an underwater video recorder (GoPro) in May 2016. In this survey, bathymetric data were used to designate sampling locations to capture a range of depths across the survey area. Constrained by the practical survey conditions, videos were collected at 28 different locations around the island (Figure 2b). For stations within the MBES survey area, the horizontal positions of the ship were measured with a dual-frequency differential GPS (centimeter accuracy). For stations in the shallower areas, the horizontal positions of the dingy were measured with a beacon-aided GPS, which provides horizontal positions with an accuracy of 1–2 m. During the video sampling, the video recorder (tied to a plumb and a float ball) was dropped to the seafloor from the static ship. Thus, considering the depth of the seafloor as well as the condition of the current, it was assumed that the uncertainty of sample location should be less than 3 m. For each station, the period of the video recording ranged from 0.5 to 3 min. Afterward, the attributes of the seafloor in these stations were categorized into four groups by visual review, according to the coral abundance levels [rare (<5% cover), low (5–30%), medium (30–60%), and high abundance (>60%)].

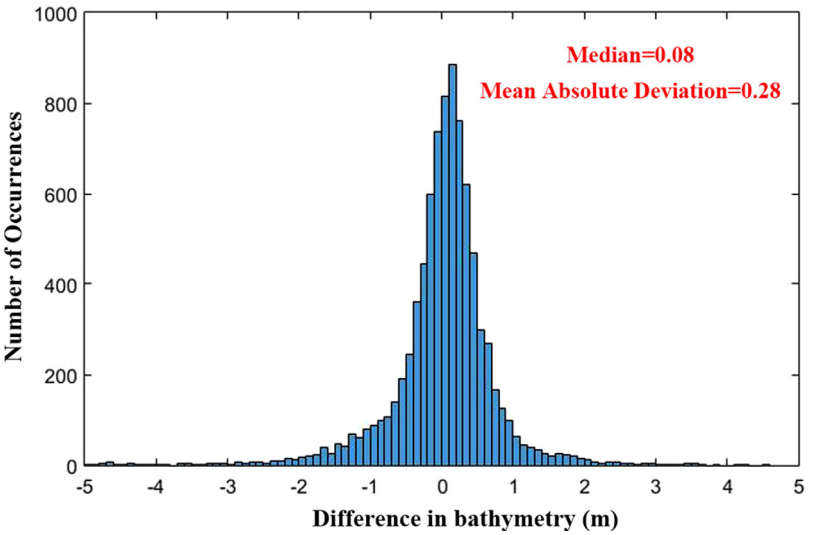

Figure 4. Histogram of the vertical difference between the MBES and lidar data on the merging edge.

3. Methodology

3.1. Benthic Habitat Mapping Based on Morphological Study

Using the merged data set, an almost seamless bathymetric data set spanning the coral reef can be obtained. Based on this data, information of terrain complexity can be derived. Terrain complexity is a fundamental ecological factor for coral reefs that is related to species diversity and richness [*Brock et al*., 2006]. Specifically, the degree of terrain complexity has a strong influence on water flow, species diversity, nutrient uptake and wave-energy dissipation [*Frost et al*., 2005; *Zawada et al*., 2010]. For these reasons, terrain complexity has frequently been used to study coral reef ecosystems [*Dunn and Halpin*, 2009; *Guinan et al*., 2009; *Pittman et al*., 2009; *Zieger et al*., 2009; *Leon et al*., 2015].

Though there is a general agreement about the importance of terrain complexity as a measure of coral habitat complexity, there is no standard measurement approach to quantify it [*Frost et al*., 2005; *Lecours*, 2016a]. In contrast, various parameterization methods have been proposed for benthic habitat mapping applications, the detailed discussion of which can be found in *Wilson et al*. [2007] and *Lecours et al*. [2016a,2016b]. In this study, our focus was to investigate the proper parameterization of terrain variability, which better accommodates the irregular terrain features of coral reef environments, as well as the inherent depth-dependent pattern of the measurement noise. Bearing these considerations in mind, the surface roughness (SR) index proposed by *Hollaus et al*. [2011] was chosen to characterize the seafloor morphology related to the coral abundance in this study.

The SR index is a parameter based on the standard deviation (STD) statistic of the local seafloor terrain. More specifically, for the bathymetric data in a window of $n \times n$ pixels (gridded DEM) (Figure 5a), a plane is used to fit the terrain points on the pixels. This derived fitted plane is used to represent the slope trend of the local bathymetry. Afterward, the residual vector is obtained by computing the orthogonal distances between the terrain points and the fitted plane. Finally, the STD of the residual vector is used to describe the terrain variability (Figure 5b).

There are two reasons for choosing such a STD-based parameterization to measure terrain complexity. First, by fitting the trend of the local terrain with a plane and then calculating the residuals relative to the fitted plane, the SR index efficiently decouples the terrain roughness from the terrain slope [*Hollaus et al*., 2011]. As a result, a better discrimination of the relationship between the true variable region and the sloping but smooth region can be obtained. This delineation is helpful for distinguishing a smooth but sloping terrain feature from the actual terrain roughness corresponding to a coral abundance area. Second, the STD statistic is a simple and straightforward measure of terrain complexity. Under this simple framework, the relationship between the noise and the actual terrain complexity is clear and explicit. Specifically, the contributions

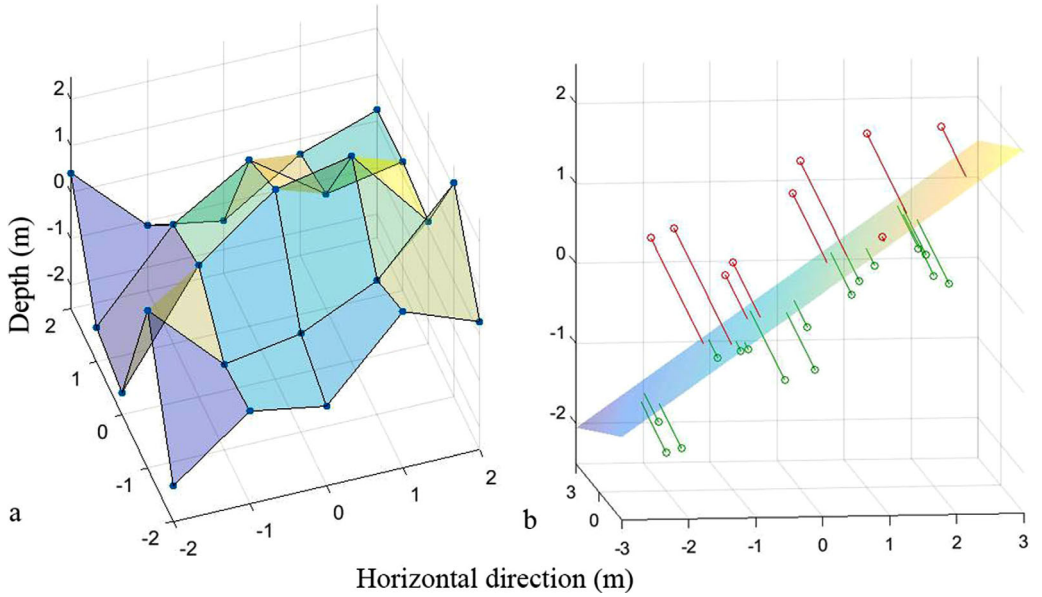

Figure 5. Schematic illustration of SR calculation. (a) Grids in a 5 × 5 local window for plane fitting. (b) SR value is derived by computing the STD of the residuals (i.e., the orthogonal distances between the terrain points and the fitted plane).

of these two factors exist in a simple, additive relation. This simple relationship makes the elimination of the depth-dependent component of the noise rather convenient, as will be shown in section 3.3.

3.2. Robust Estimation of the Local Terrain Slope

When trying to use the SR index to measure terrain complexity, the first challenge is to account for the irregularity of the seafloor. Traditionally, when computing a SR value for a local window, the least squares (LS) regression is used to fit the terrain points to capture the main trend of the local terrain. However, the LS regression is known for its inefficiency in a non-Gaussian environment. The bathymetry of the coral reef is a typical case of a non-Gaussian environment, where the distribution of the terrain is highly variable and irregular. Consequently, the fitted plane could seriously deviate from the actual trend of the local terrain, which would result in a biased SR estimate. Thus, a different approach is required to accurately describe the trend of the irregular bathymetry in the local window.

When considering an irregular terrain feature, one basic observation is that a small portion of the irregular terrain points in a local window can be regarded as outliers from a statistical viewpoint. Therefore, to address the problem stated above, a robust estimation procedure is used to fit a plane to the local terrain points. Specifically, the least median square (LMS) regression is used to fit the terrain. By substituting the LS criterion with the LMS criterion, the regression possesses a higher resistance to outliers but a lower estimation efficiency [*Rousseeuw*, 1984]. As a result, a robust but inefficient initial fitting is obtained. Using the estimate obtained from the LMS regression as an initial value, the M-estimator proposed by *Huber* [2011] is then executed. Using this two-step procedure, an accurate and robust estimation solution can be obtained.

3.3. Depth Calibration of the SR Estimate

After robustly estimating the trend of the local terrain, the second challenge in accurately computing the SR index is to cope with the depth-dependent patterns of the measurement noise. An inherent feature of the bathymetric data is that the accuracy of the measurements decreases as the water depth increases (for both lidar and MBES data). To depict this linear relationship, following International Hydrographic Organization (IHO) standards, the vertical accuracy of a bathymetric measurement is evaluated by introducing a depth-dependent factor b:

$$E_b(95\%) = \sqrt{a^2 + (b \cdot d)^2} \tag{1}$$

where a is the depth-independent error, b is the depth-dependent factor and d is the depth [*International Hydrographic Organisation* (*IHO*), 2008]. Thus, if the impact of this depth-dependent pattern is not

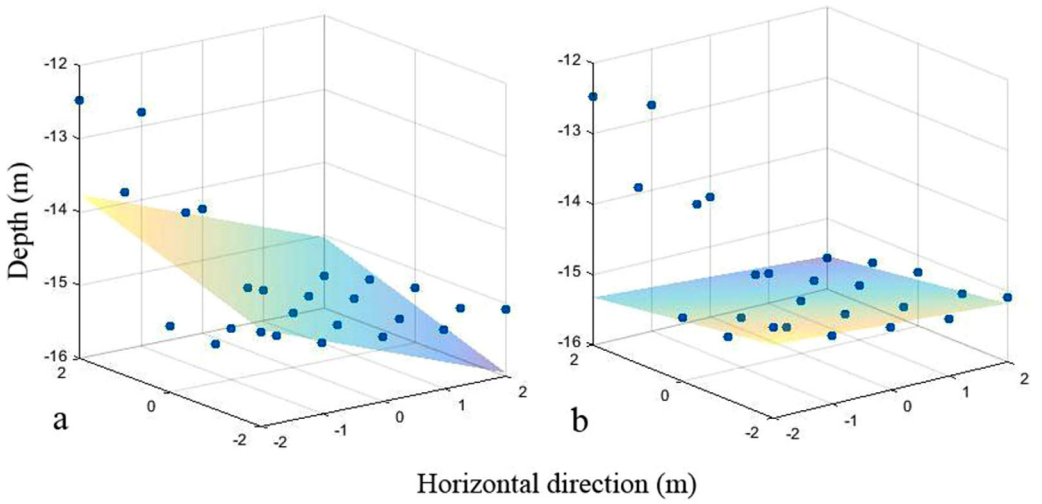

Figure 6. Comparison of the LS regression and the robust estimation in irregular bathymetry environments (extracted from lidar data set). (a) LS regression result. (b) Robust estimation result.

addressed, the computed SR index will be influenced by variations in depth. To be more specific, in deep-sea areas, even when the seafloor is very smooth, a large SR value could be obtained due to an increase in noise at depth. To address this problem, the SR index is calibrated according to its corresponding depth. Following the IHO standards, a depth-dependent factor b_c is introduced in the computation:

$$SR_c = \sqrt{\max\left[0, SR^2 - \left(b_c \cdot \bar{d} \cdot \cos(\theta)\right)^2\right]} \tag{2}$$

where SR_c is the calibrated SR index and $\bar{d}$ and θ are the mean depth and the slope of the local seafloor patch, respectively. Under the square root sign in this equation, the correction term is simply chosen to be $\left(b_c \cdot \bar{d} \cdot \cos(\theta)\right)^2$. This setting is chosen because the contributions of the actual terrain features and the noise are simply additive under the STD framework (or equivalently, under the variance framework). Therefore, once the factor b_c is fixed, its contribution can be eliminated by simple subtraction. After the above calibration, the depth-dependent component of the measurement noise is accounted for, and the SR indexes with different depths are fixed to the same benchmark.

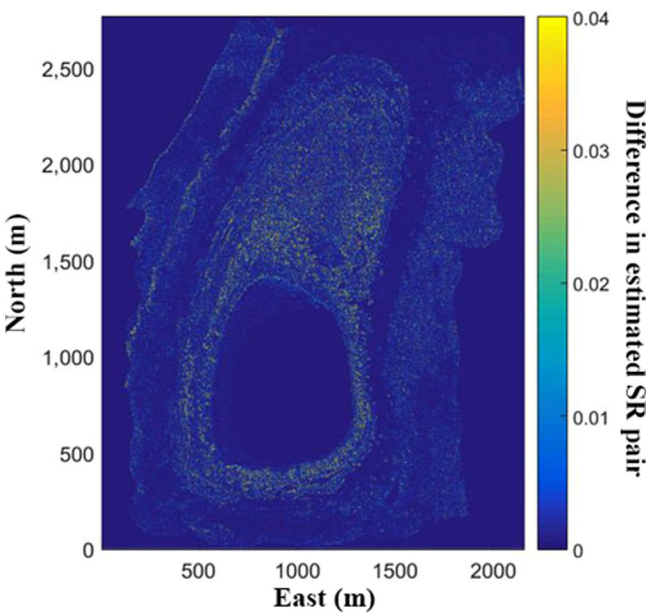

Figure 7. Spatial distribution of the differences between SR_R and SR_{LS}.

4. Results

Throughout this study, the SR index was calculated using a gridded DEM (1 m resolution). In the computation, the size of the local window was chosen to be 5 × 5 pixels.

First, the effect of using the robust estimation procedure in the coral reef bathymetry environment was investigated. Figure 6 highlights the necessity of applying the robust estimation in a typical irregular region, where the local bathymetry (in a 5 × 5 local window) is highly variable. As shown in Figure 6a, the LS regression is highly sensitive to the irregular parts of the local bathymetry. Consequently, the fitted

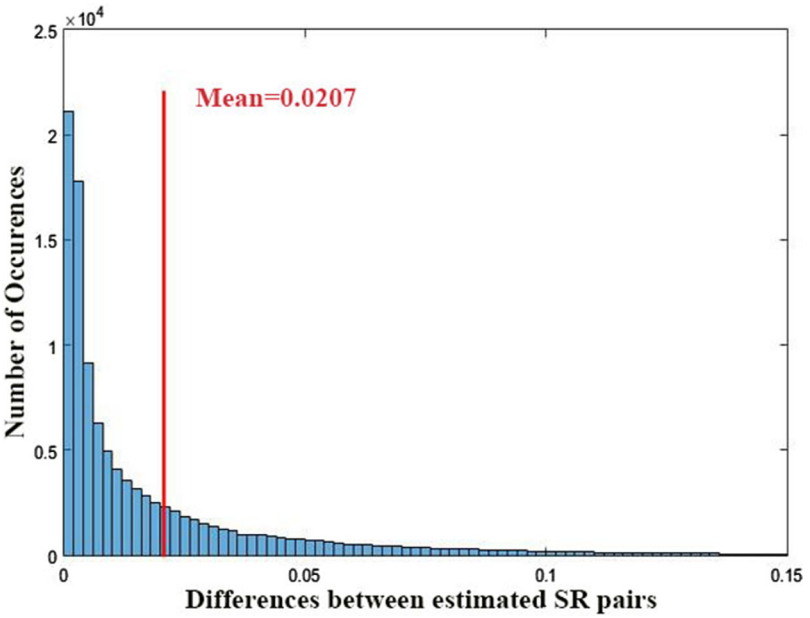

Figure 8. Histogram of D_{SR} (when $SR_{LS} > 0.3$).

plane obviously deviates toward the irregular terrain points, resulting in a biased estimate of the slope's trend. However, with the robust regression, the main trend of the slope in this local region is well captured (Figure 6b), which is critical for accurately estimating the SR index. To evaluate the impact of this difference in the slope trend estimates, the local window was applied to the whole merged data set, and the SR values from both estimation methods were compared. In total, 3,998,035 pairs of SR values were obtained. In most

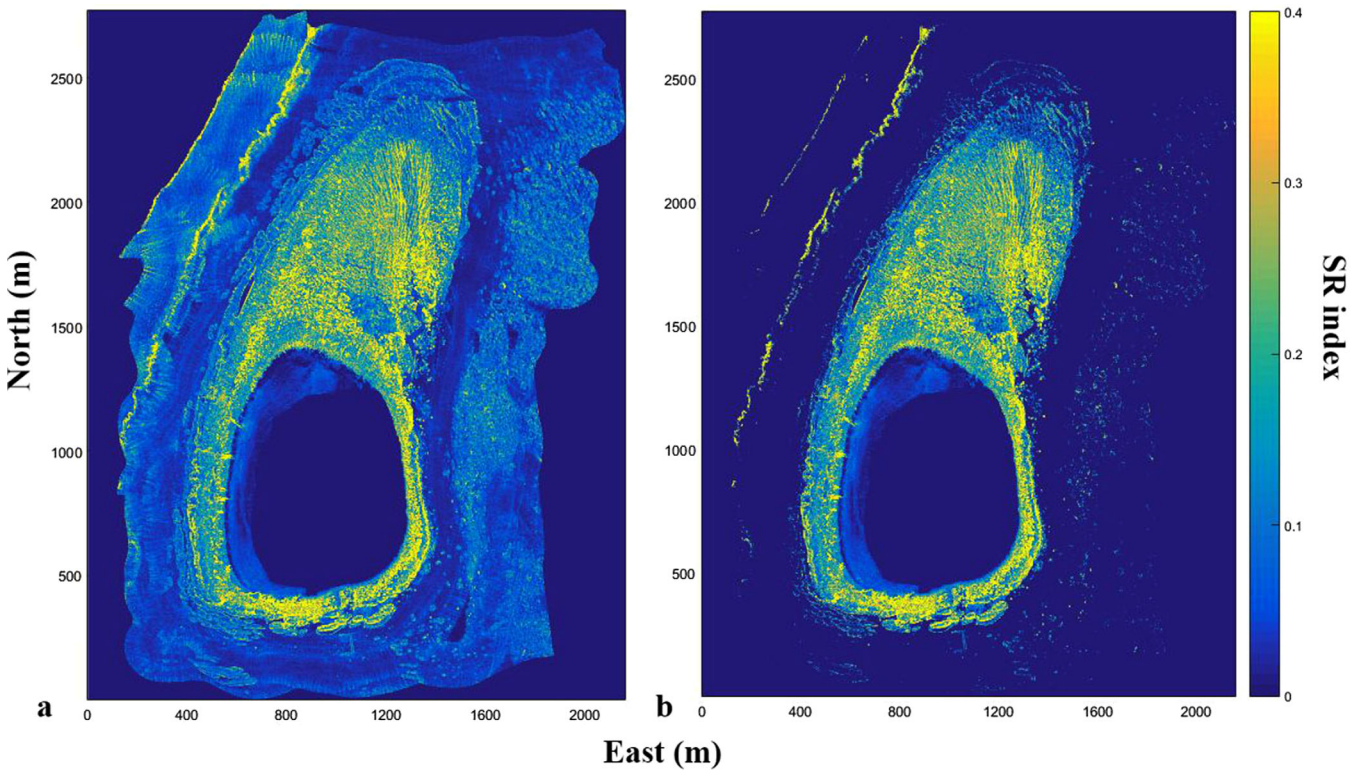

Figure 9. Spatial distribution of the SR index. (a) Without depth calibration. (b) With depth calibration.

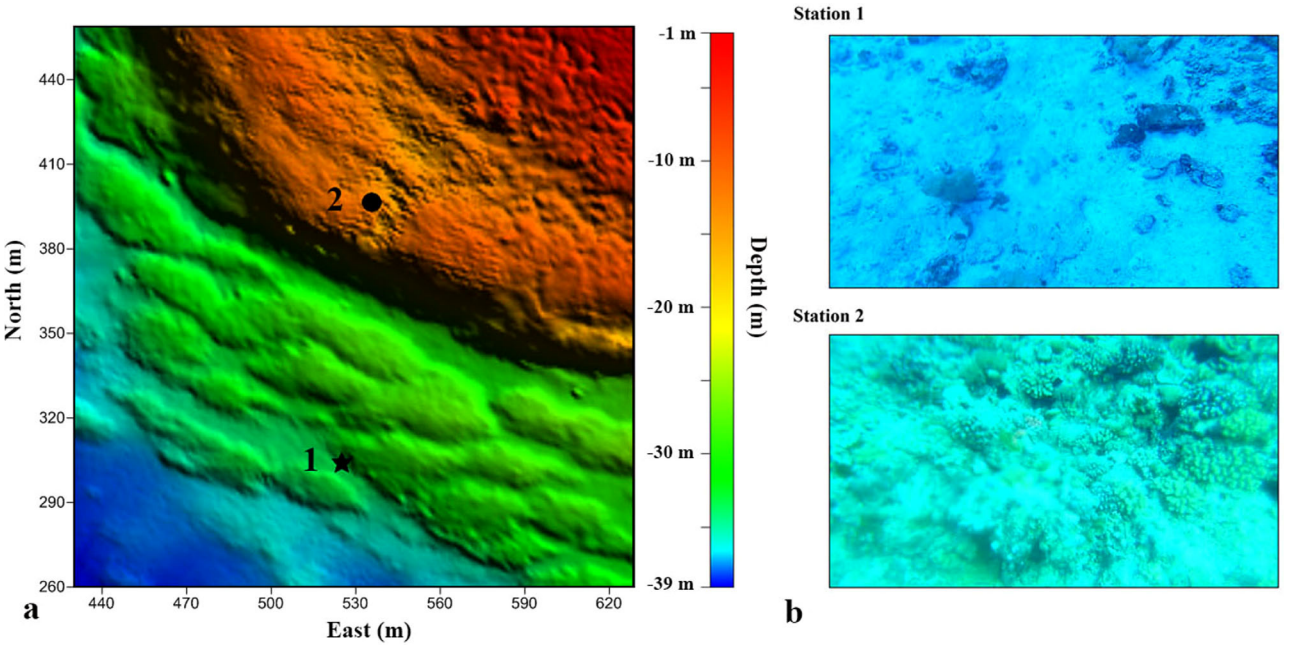

Figure 10. DEM of a smaller area. (a) Shaded relief image of the seafloor bathymetry of the selected area. (b) Representative pictures of two ground-truth stations.

of these pairs, the robust procedure was found to give a larger SR estimate than the LS regression. Figure 7 shows the spatial distribution of the differences between the SR values (D_{SR}) obtained using the robust procedure (SR_R) and the regular procedure (SR_{LS}). For most of the region, D_{SR} is negligible. Obviously, this corresponds to the regular terrain region of the seafloor. In areas with larger terrain differences (and thus larger SR values), the robust procedure tends to show a more notable difference. Figure 8 shows the histogram of the D_{SR} values when the SR_{LS} values are larger than 0.3. In regions with such irregular bathymetry, the differences between the two methods become significant. Thus, it can be deduced that the regular regression tends to underestimate the level of terrain complexity in irregular bathymetry environments compared to the robust estimation.

Using the robust estimation procedure, the SR index over the whole study area was determined and is shown in Figure 9, which reveals abundant morphological features. Using manual interpretation, the obvious morphological features of coral can be observed in the shallow-water region (the middle part of the study area where the depth is less than 20 m). In addition, these morphological features are also evident in the eastern part

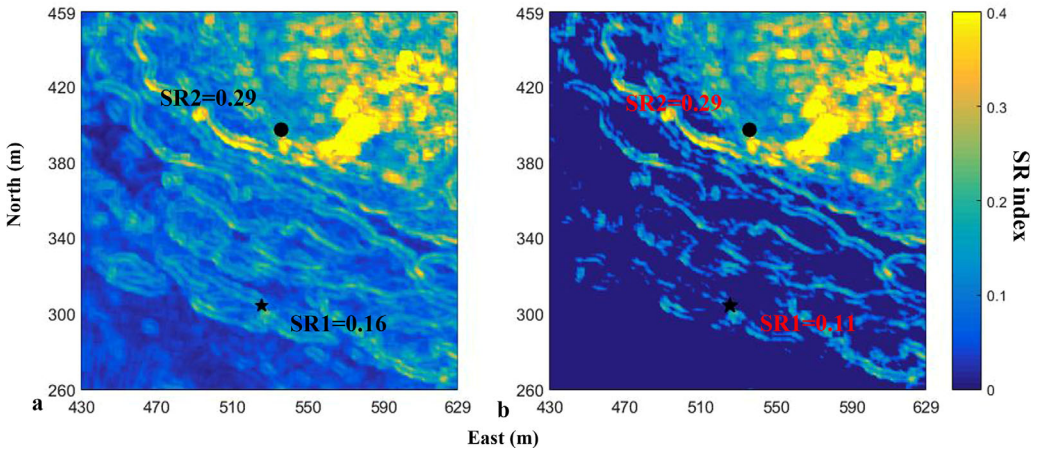

Figure 11. Spatial distribution of the SR index. (a) Without depth calibration. (b) With depth calibration.

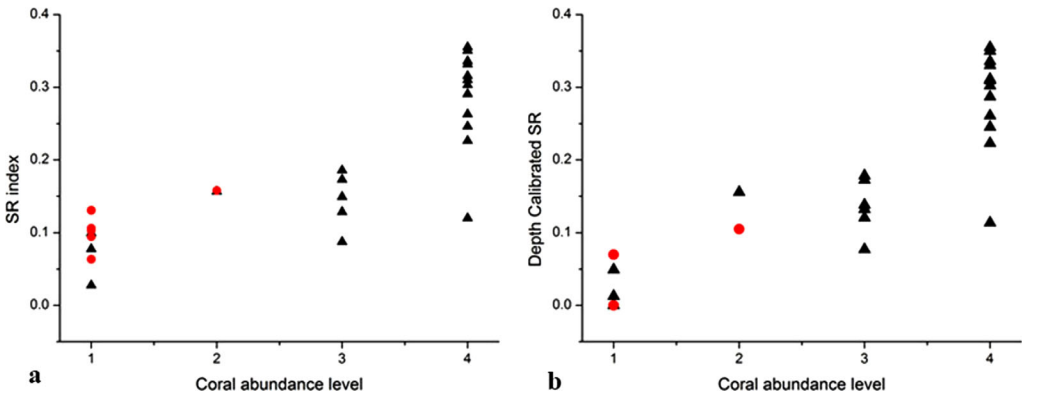

Figure 12. Statistical relationship between the SR index and coral abundance, where the red circles denote stations with depths >15 m. (a) Without depth calibration. (b) With depth calibration.

of the study area (with the depths of 30–40 m). Along with these interesting features, the existence of the depth-dependent pattern is also evident. In particular, the ribbing artifacts [*Hughes-Clarke*, 2003], which are induced by inaccurate attitude measurements, are obvious in deep areas (i.e., the western part of the study area). To overcome these interferences, a depth-dependent factor b_c of 0.00375 (the special order of IHO standards) [*IHO*, 2008] was introduced into equation (2) to calibrate the SR index (Figure 6b). After the calibration, the depth-dependent interferences in deep areas were largely eliminated. In contrast, in the middle and eastern regions of the study area, the majority of the high SR values were retained. Obviously, the spatial distribution pattern of the SR index in the study area was changed remarkably by the depth calibration. To better illustrate the performance of the different methods, the computed results of a local area are presented. The dimensions of the local area are 200 m by 200 m, with two video stations (Figure 10). Figure 11 compares the performance of the robust estimation with and without the depth calibration. As shown in the figure, after the calibration, there is better agreement between the estimated SR values and the corresponding coral abundance levels.

Third, the relationship between the obtained SR index and the actual level of coral abundance was evaluated. Figure 12a shows the relationship between the two variables before the depth calibration described above. Generally, the SR indexes increase with an increase in the coral abundance level. In addition, the Spearman rank correlation results demonstrated strong positive correlations between the SR index and coral abundance ($r = 0.82$, $P < 0.001$). The relationship between the two variables after the depth calibration was also examined (Figure 12b). Obviously, for stations with depths exceeding 15 m (red circles), the SR values were reduced by the calibration. This reduction was found to be in agreement with the corresponding coral abundance levels. This agreement was further confirmed by the increase in the Spearman rank correlation coefficient ($r = 0.89$, $P < 0.001$). Thus, it can be concluded that accounting for the depth-dependent disturbance in bathymetric measurements increases the significance of the relationship between the SR index value and the coral abundance.

5. Discussion

This study focused on providing an effective morphological method for mapping coral abundance based on combined bathymetric data from lidar and MBES measurements. According to the experimental results in section 4, the following statements can be made.

1. The complexity of the bathymetry has important implications for the coral abundance on the seafloor. Basically, seafloor complexity plays an important role in the growth process of coral. Moreover, bathymetric complexity is also a representation of a high-level substrate complexity. In general, reasons for this bathymetric complexity include the presence of rocks, gravel or human deposits on the seafloor or the presence of benthic habitats, such as coral reefs or underwater plants. However, in remote coral atoll environments, where rocks and human deposits are rare, the relationship between terrain complexity and benthic habitats becomes much more significant. In particular, because underwater plants are seldom observed in the region around Yuanzhi Island, the terrain complexity becomes a reliable indicator of coral abundance.

2. Terrain features on the seafloor are often highly irregular, especially in coral reef regions. Consequently, a traditional LS regression is unsuitable for fitting the trends in these areas, due to their deviation from a Gaussian noise distribution. From a statistical perspective, terrain irregularity points in a local window can be regarded as outliers. Hence, robust estimation is applied to fit the local seafloor trend. Based on the initial estimate provided by the LMS regression, the M estimator is executed to obtain a robust and accurate estimate of the slope trend for each grid point on the seafloor. Compared to the traditional LS regression, the robust estimation tends to generate a larger SR value. The reason for this difference is that the LS regression is quite sensitive to irregular terrain points. As shown in Figure 6a, the estimated plane is strongly influenced by irregular points. Thus, a smaller square of residuals is obtained, resulting in an underestimate of the SR index. This underestimation becomes more significant in areas with more variable terrain (Figure 8). Obviously, the impact of this underestimate is not insignificant since the majority of the SR indexes range between 0 and 0.4 (Figure 9). Therefore, in order to accurately measure the complexity level of the bathymetry, it is necessary to address the impact of irregular terrain with robust estimations.
3. Lidar and MBES measurements are complementary when surveying the bathymetry of coral reefs. Using their complementary coverage of different depth regions, an approximately seamless measurement of coral reef bathymetry can be obtained. A notable feature of this measurement is the depth-dependent pattern of its uncertainty (for both lidar and MBES data). This pattern means that the calculated SR values increase with depth. As such, a depth-dependent factor is introduced to eliminate the impact of the depth-dependent uncertainty. Nevertheless, for a particular survey environment, an accurate estimation of the depth-dependent factor is seldom available. In a smooth seafloor environment, the factor b_c can be estimated by examining the statistical relationship between the bathymetric complexity and depth. However, in a coral reef environment, such attempts are made difficult by the highly variable terrain features resulting from the existence of coral. Therefore, as a conservative estimate, the quantification of b_c directly follows the suggestion of the IHO standards (special order). As shown in Figure 9, the depth-dependent interferences were largely eliminated. In addition, the SR indexes for different depths were fixed to the same benchmark, which is a necessary step for accurately judging the coral abundance level. These techniques allow the relationship between the computed SR index and the in situ coral abundance observations to become more statistically significant.

6. Conclusion

In this study, one major goal was to explore the potential for the accurate characterization of coral reefs using morphological studies of the bathymetry. To this end, this study focused on a method for effectively measuring the terrain complexity of a coral reef. In the developed method, the disturbance of terrain irregularities is accounted for by robust estimation. Meanwhile, a depth calibration procedure was introduced to eliminate the disturbance of the depth-dependent noise component. As suggested by the experimental results, the presented method provides better characterization of the seafloor terrain complexity. Meanwhile, the obtained SR index was found to be significantly correlated with the in situ coral abundance observations, which suggests that the SR index is a suitable indicator of habitat complexity in a coral reef environment. Although the study area in this research was limited to the Yuanzhi Island, the methods are assumed to be capable of generalizing to other coral reef regions in the world.

Acknowledgments

This work was supported by the National Natural Science Foundation of China (41506111, 41376108), and the Public science and technology research funds projects of surveying, mapping and geoinformation (201512034). The highly valuable comments made by the editor and two anonymous reviewers are acknowledged. The data used in this study are available at (https://figshare.com/articles/Morphological_characterization_of_coral_reefs_by_combining_LiDAR_and_MBES_data_a_case_study_from_Yuanzhi_Island_South_China_Sea/4985555).

References

Anderson, J. T., D. Van Holliday, R. Kloser, D. G. Reid, and Y. Simard (2008), Acoustic seabed classification: Current practice and future directions, *ICES J. Mar. Sci.*, *65*(6), 1004–1011.

Brock, J. C., and S. J. Purkis (2015), The emerging role of lidar remote sensing in coastal research and resource management, *J. Coastal Res.*, *25*(6), 1–5.

Brock, J. C., C. W. Wright, I. B. Kuffner, R. Hernandez, and P. Thompson (2006), Airborne lidar sensing of massive stony coral colonies on patch reefs in the northern Florida reef tract, *Remote Sens. Environ.*, *104*, 31–42.

Collier J. S., and S. R. Humber (2007), Time-lapse side-scan sonar imaging of bleached coral reefs: A case study from the Seychelles, *Remote Sens. Environ.*, *108*(4), 339–356.

Collin A., B. Long, and P. Archambault (2012), Merging land-marine realms: Spatial patterns of seamless coastal habitats using a multispectral LiDAR, *Remote Sens. Environ.*, *123*, 390–399.

Costa, B. M., T. A. Battista, and S. J. Pittman (2009), Comparative evaluation of airborne LiDAR and ship-based multibeam SoNAR bathymetry and intensity for mapping coral reef ecosystems, *Remote Sens. Environ.*, *113*(5), 1082–1100.

Dunn, D. C., and P. N. Halpin (2009), Rugosity-based regional modeling of hard-bottom habitat, *Mar. Ecol. Prog. Ser.*, *377*, 1–11.

Frost, N. J., M. T. Burrows, M. P. Johnson, M. E. Hanley, and S. J. Hawkins (2005), Measuring surface complexity in ecological studies, *Limnol. Oceanogr. Methods*, *3*, 203–210.
Guinan, J., A. J. Grehan, M. F. Dolan, and C. Brown (2009), Quantifying relationships between video observations of cold-water coral cover and seafloor features in Rockall Trough, west of Ireland, *Mar. Ecol. Prog. Ser.*, *375*, 125–138.
Hedley, J. D., C. M. Roelfsema, I. Chollett, A. R. Harborne, S. F. Heron, S. Weeks, and V. Ticzon (2016), Remote sensing of coral reefs for monitoring and management: A review, *Remote Sens.*, *8*(2), 118.
Hollaus, M., C. Aubrecht, H. Bernhard, K. Steinnocher, and W. Wagner (2011), Roughness mapping on various vertical scales based on full-waveform airborne laser scanning data, *Remote Sens.*, *3*(3), 503–523.
Huber, P. J. (2011), *Robust Statistics*, Springer, Berlin.
Hughes-Clarke, J. E. (2003), Dynamic motion residuals in swath sonar data: Ironing out the creases, *Int. Hydrol. Rev.*, *4*(1), 1–30.
Ierodiaconou, D., A. Rattray, J. Monk, L. Laurenson, and V. Versace (2011), Comparison of automated classification techniques for predicting benthic biological communities using hydroacoustics and video observations, *Cont. Shelf Res.*, *31*, 28–38.
International Hydrographic Organisation (IHO) (2008), *IHO Standards for Hydrographic Surveys*, *Spec. Publ. 44*, 5th ed., Int. Hydrogr. Bur., Monaco, France.
Jenness, J. (2002), *Surface Areas and Ratios from Elevation Grid (surfgrids.avx) Extension for ArcView 3.x—Version 1.2*, Jenness Enterprises, Flagstaff, Ariz. [Available at http://www.jennessent.com/arcview/grid tools.htm.]
Kennedy, D. M., D. Ierodiaconou, and A. Schimel (2014), Granitic coastal geomorphology: Applying integrated terrestrial and bathymetric LiDAR with multibeam sonar to examine coastal landscape evolution, *Earth Surf. Processes Landforms*, *39*(12), 1663–1674.
Lecours, V., M. F. Dolan, A. Micallef, and V. L. Lucieer (2016a), A review of marine geomorphometry, the quantitative study of the seafloor, *Hydrol. Earth Syst. Sci.*, *20*(8), 3207–3244.
Lecours, V., M. F. Dolan, A. Micallef, and V. L. Lucieer (2016b), Characterising the ocean frontier: A review of marine geomorphometry, *Hydrol. Earth Syst. Sci.*, 1–66.
Leon, J. X., C. M. Roelfsema, M. I. Saunders, and S. R. Phinn (2015), Measuring coral reef terrain roughness using 'Structure-from-Motion' close-range photogrammetry, *Geomorphology*, *242*, 21–28.
Lurton, X. (2010). *An Introduction to Underwater Acoustics*, Springer, London.
Micallef, A., T. P. Le Bas, V. A. Huvenne, P. Blondel, V. Hühnerbach, and A. Deidun (2012), A multi-method approach for benthic habitat mapping of shallow coastal areas with high-resolution multibeam data, *Cont. Shelf Res.*, *39*, 14–26.
Mishra, D. R., S. Narumalani, D. Rundquist, M. Lawson, and R. Perk (2007), Enhancing the detection and classification of coral reef and associated benthic habitats: A hyperspectral remote sensing approach, *J. Geophys. Res.*, *112*, C08014, doi:10.1029/2006JC003892.
Pittman, S. J., and K. A. Brown (2011), Multi-scale approach for predicting fish species distributions across coral reef seascapes, *PloS One*, *6*(5), e20583.
Pittman, S. J., B. M. Costa, and T. A. Battista (2009), Using lidar bathymetry and boosted regression trees to predict the diversity and abundance of fish and corals, *J. Coastal Res.*, *SI*(53), 27–38.
Reshitnyk, L., M. Costa, C. Robinson, and P. Dearden (2014), Evaluation of WorldView-2 and acoustic remote sensing for mapping benthic habitats in temperate coastal Pacific waters, *Remote Sens. Environ.*, *153*, 7–23.
Rousseeuw, P. J. (1984), Least median of squares regression, *J. Am. Stat. Assoc.*, *79*(388), 871–880.
Tulldahl, H. M., and S. A. Wikström (2012), Classification of aquatic macrovegetation and substrates with airborne lidar, *Remote Sens. Environ.*, *121*, 347–357.
Wang, C. K., and W. D. Philpot (2007), Using airborne bathymetric lidar to detect bottom type variation in shallow waters, *Remote Sens. Environ.*, *106*(1), 123–135.
Wedding, L. M., A. M. Friedlander, M. McGranaghan, R. S. Yost, and M. E. Monaco (2008), Using bathymetric lidar to define nearshore benthic habitat complexity: Implications for management of reef fish assemblages in Hawaii, *Remote Sens. Environ.*, *112*(11), 4159–4165.
Wilson, M. F., B. O'Connell, C. Brown, J. C. Guinan, and A. J. Grehan (2007), Multiscale terrain analysis of multibeam bathymetry data for habitat mapping on the continental slope, *Mar. Geod.*, *30*(1–2), 3–35.
Xu, L. Q., X. D. Liu, L. G. Sun, H. Yan, Y. Liu, Y. H. Luo, and J. Huang (2011), Geochemical evidence for the development of coral island ecosystem in the Xisha Archipelago of South China Sea from four ornithogenic sediment profiles, *Chem. Geol.*, *286*, 135–145.
Yamamoto, K. H., R. L. Powell, S. Anderson, and P. C. Sutton (2012), Using LiDAR to quantify topographic and bathymetric details for sea turtle nesting beaches in Florida, *Remote Sens. Environ.*, *125*, 125–133.
Young M., D. Ierodiaconou, and T. Womersley (2015), Forests of the sea: Predictive habitat modelling to assess the abundance of canopy forming kelp forests on temperate reefs, *Remote Sens. Environ.*, *170*, 178–187.
Zavalas, R., D. Ierodiaconou, D. Ryan, A. Rattray, and J. Monk (2014), Habitat classification of temperate marine macroalgal communities using bathymetric LiDAR, *Remote Sens.*, *6*(3), 2154–2175
Zawada, D. G., G. A. Piniak, and C. J. Hearn (2010), Topographic complexity and roughness of a tropical benthic seascape, *Geophys. Res. Lett.*, *37*, L14604, doi:10.1029/2010GL043789.
Zieger, S., T. Stieglitz, and S. Kininmonth (2009), Mapping reef features from multibeam sonar data using multiscale morphometric analysis, *Mar. Geol.*, *264*(3), 209–217.